

^7Be , $^8\text{B}+$ ^{208}Pb Elastic Scattering at Above-Barrier Energies

This content has been downloaded from IOPscience. Please scroll down to see the full text.

2013 J. Phys.: Conf. Ser. 420 012075

(<http://iopscience.iop.org/1742-6596/420/1/012075>)

View [the table of contents for this issue](#), or go to the [journal homepage](#) for more

Download details:

IP Address: 60.170.126.206

This content was downloaded on 31/10/2015 at 02:58

Please note that [terms and conditions apply](#).

${}^7\text{Be}$, ${}^8\text{B}+{}^{208}\text{Pb}$ Elastic Scattering at Above-Barrier Energies

J.S. Wang^{1,*}, Y.Y. Yang^{1,2}, Q. Wang¹, L. Jin^{1,2}, J.B. Ma¹,
M.R. Huang¹, J.L. Han¹, P. Ma¹, S.L. Jin^{1,2}, Z. Bai^{1,2}, Q. Hu^{1,2},
J.B. Chen^{1,2}, R. Wada¹, Z.Y. Sun¹, R.F. Chen¹, X.Y. Zhang¹,
Z.G. Hu¹, X.H. Yuan¹, X.G. Cao¹, Z.G. Xu¹, S.W. Xu¹, C. Zhen¹,
Z.Q. Chen¹, Z. Chen^{1,2}, S.Z. Chen^{1,2}, C.M. Du^{1,2}, L.M. Duan¹, F. Fu¹,
B.X. Gou^{1,2}, J. Hu¹, J.J. He¹, X.G. Lei¹, S.L. Li¹, Y. Li^{1,2}, Q.Y. Lin^{1,2},
L.X. Liu^{1,2}, F.D. Shi¹, S.W. Tang^{1,2}, G. Xu^{1,2}, L.Y. Zhang^{1,2},
X.H. Zhang¹, W. Zhang^{1,2}, M.H. Zhao^{1,2}, Y.H. Zhang¹, H.S. Xu¹,
G.Q. Xiao¹, S. Mukhejee³, N. Keeley⁴, K. Rusek^{4,5}, D.Y. Pang⁶

¹ Institute of Modern Physics, Chinese Academy of Sciences, Lanzhou, 730000, China.

² Graduate University of Chinese Academy of Sciences, Beijing, 100049, China.

³ Physics Department, Faculty of Science, M.S. University of Baroda, Vadodara - 390002, India.

⁴ National Centre for Nuclear Research, ul. Andrzejka Soltana 7, 05-400 Otwock, Poland.

⁵ Heavy Ion Laboratory, University of Warsaw, ul. Pasteura 5A, PL-02-093 Warsaw, Poland.

⁶ School of Physics and Nuclear Energy Engineering, Beihang University, Beijing 100191, China.

E-mail: jswang@impcas.ac.cn

Abstract. Angular distributions for the elastic scattering of ${}^7\text{Be}$ and ${}^8\text{B}$ by an enriched ${}^{208}\text{Pb}$ target were measured at the Radioactive Ion Beam Line at Lanzhou (RIBLL). The incident energies of the radioactive beams were about three times the respective Coulomb barriers. A suppressed Coulomb-nuclear Interference Peak (CNIP) is not observed for ${}^8\text{B}$, a pronounced proton halo nucleus. Optical model fits were performed using Woods-Saxon potentials and the total reaction cross sections deduced. The results are discussed.

1. Introduction

Weakly-bound nuclei have been extensively studied with the development of radioactive ion beam facilities since the 1980s [1]. Many interesting phenomena have been discovered by studying the weakly-bound nuclei close to the proton/neutron drip-lines, such as neutron/proton halo/skin structures, evolution of shell structure with N/Z ratio, exotic modes of collective excitation etc. [2, 3, 4, 5].

Halo nuclei, composed of a compact core and extended valence nucleons, have small separation energies and the valence nucleons are located in orbitals with low angular momentum. This halo structure should affect dramatically the mechanism of breakup, transfer and fusion reactions [6]. A study of the elastic scattering of the neutron halo nucleus ${}^6\text{He}$ by ${}^{208}\text{Pb}$ near the Coulomb barrier shows the existence of a sizeable long range absorption mechanism in the optical model potential [7, 8]. An experimental study of another neutron halo nucleus, ${}^{11}\text{Be}$, at energies

around the Coulomb barrier found that the CNIP disappears and absorption occurs at much smaller angles than for the other Be isotopes, $^9,^{10}\text{Be}$ [9]. This unusual behaviour is caused by the strong nuclear coupling to the continuum in ^{11}Be [10]. An accurate measurement of the elastic scattering differential cross section is very important for the determination of the optical potential parameters and the so-called quarter-point angle ($\theta_{1/4}$) [11].

It is known that ^8B is a well-pronounced proton halo nucleus. The binding energy of the last proton is only 0.137 MeV. Much research has been done on ^8B by measuring the total reaction cross section, breakup cross section, fusion cross section and inelastic scattering differential cross section [12, 13, 14, 15, 16, 17, 18]. However, experimental data for elastic scattering of ^8B by heavy targets are scarce [19]. The only elastic scattering data for ^8B by light and intermediate mass targets are in refs. [20, 21, 22]. The proton halo effects are manifest in the total reaction cross sections deduced from the experimental data. In this contribution we present new elastic scattering data for ^7Be and ^8B from the heavy target ^{208}Pb , which were measured at RIBLL at the Institute of Modern Physics, Chinese Academy of Sciences [24, 25], at incident energies about three times the Coulomb barrier.

2. Experimental setup

The unstable nuclear beams of 17.9 MeV/A ^7Be and 21.3 MeV/A ^8B were produced by RIBLL. A 54.2 MeV/A ^{12}C primary beam was accelerated by the Heavy Ion Research Facility of Lanzhou (HIRFL) and delivered to a 2615 μm thick Be primary target. The secondary beams were separated and purified by RIBLL. The intensity of the ^8B secondary beam was a few hundred particles per second with a primary beam intensity of ~ 300 enA, while that of the ^7Be beam was ~ 5000 particles per second.

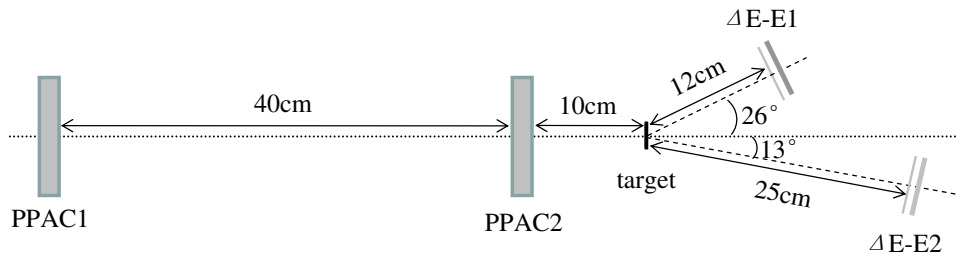


Figure 1. Schematic view of the experimental setup.

The experimental setup is shown in Fig. 1. The secondary target was 4.2 mg/cm^2 thick enriched ^{208}Pb . Two fast scintillator detectors were placed at the two focal planes of the RIBLL at a distance of 17 m apart as a time of flight measurement. Combining with the ΔE detector and the magnetic rigidity setting, the secondary particles were clearly identified. The position and direction of the incident particles on the target were determined by two position-sensitive Parallel-Plate Avalanche Counter (PPAC) detectors with active area $80 \times 80 \text{ mm}^2$ and position resolution about 1 mm in both X and Y directions. Fig. 2 shows a typical beam profile at the two PPACs before the secondary target with the X position on the x-axis and Y position on the y-axis. The scattered particles were detected after the secondary target with two silicon-detector ΔE -E telescopes. Each telescope consisted of a 150 μm thick double-sided silicon strip detector with an active area of $48 \times 48 \text{ mm}^2$ as a ΔE detector and a 1500 μm thick silicon detector as E detector. The silicon strip detectors were perpendicularly segmented into 48 strips on both sides and the position resolution was 1 mm in both the vertical and horizontal directions.

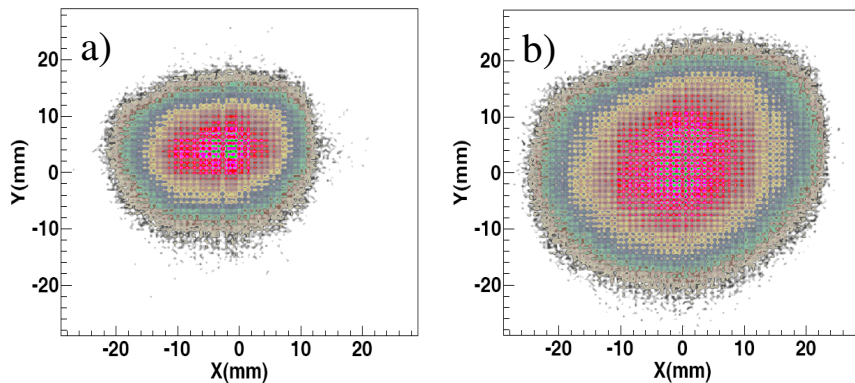


Figure 2. The secondary beam profiles.

3. Data Analysis

Data analysis for the elastic scattering of unstable beams is not easy because of a large beam spot and a larger angle of emission compared with stable beams.

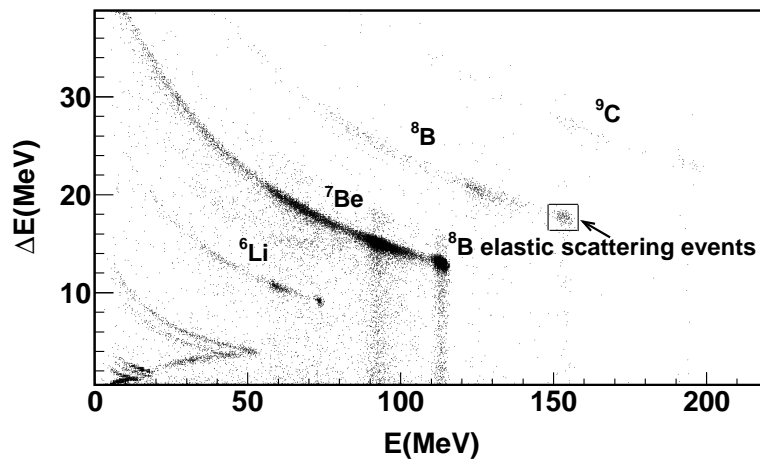


Figure 3. A typical particle identification spectrum.

The ${}^7\text{Be}$ and ${}^8\text{B}$ secondary beams were clearly separated in the TOF spectrum with the RIBLL setting at an appropriate magnetic rigidity. The elastic scattering events were identified with the ΔE - E telescopes after the secondary target (see Fig. 3). The window in Fig. 3 shows the ${}^8\text{B}$ elastic scattering events and the other two bunches of ${}^8\text{B}$ located at low energies are due to the incident ${}^8\text{B}$ beam hitting one or two of the tungsten wires in the PPACs before the secondary target. Data normalization was obtained by assuming the ${}^8\text{B}$ elastic scattering to be purely Rutherford at very forward angles. The scattering angles are calculated event-by-event, using the position information measured by the two PPACs in the beam line before the secondary target and the double-sided silicon detectors after it. The secondary beam spot on the target is almost a circle of 30 mm diameter and a non-uniform distribution. The angle of emission of the secondary beam is also large. The differential cross section is difficult to obtain from a

direct calculation of the solid angles of the strip detectors and the number of particles scattered into the detector because the position and direction of the incident beam have to be taken into account event-by-event. In order to evaluate the ratio of the elastic scattering to the Rutherford cross section, a Monte Carlo simulation was used. The actual geometry of the detector setup and the real beam distribution were taken into account in the simulation. Thus, the angular distribution of the elastic scattering cross section is obtained as the following formula.

$$\frac{d\sigma(\theta)}{d\sigma_{Ruth}(\theta)} = \frac{\frac{d\sigma(\theta)_{exp}}{d\Omega}}{\frac{d\sigma(\theta)_{Ruth}}{d\Omega}} = C \times \frac{N(\theta)_{exp}}{N(\theta)_{Ruth}} \quad (1)$$

where C is a normalization constant, which is a global normalization factor and determined by supposing that the ${}^7\text{Be}$ (${}^8\text{B}$) elastic scattering cross section is pure Rutherford scattering at very forward angles. $N(\theta)_{exp}$ and $N(\theta)_{Ruth}$ are the yields at a given angle from the experiment and the simulation respectively. This data extraction method does not require an accurate knowledge of the number of incoming particles and the target thickness. Systematic errors arising from calculation of the solid angles are avoided. Since the differential cross section is very sensitive to the scattering angle θ and a small angular deviation may result in a significant error in the measured elastic scattering cross section, a detector misalignment correction was applied, as in some other elastic scattering experiments [26].

4. Results and Brief Discussion

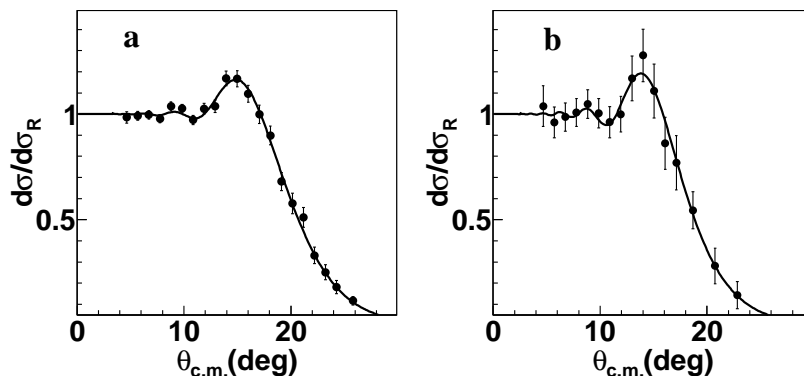


Figure 4. Angular distributions of ${}^7\text{Be}$ (a) and ${}^8\text{B}$ (b) elastic scattering from ${}^{208}\text{Pb}$ (note the linear cross section scale). The lines represent optical model fits. Error bars are statistical.

The experimental data for the elastic scattering angular distributions are shown in Fig. 4 for ${}^7\text{Be}$ (left) and ${}^8\text{B}$ (right) at centre of mass energies of 121 MeV and 164 MeV respectively. The error bars shown in the figure are mainly statistical. A CNIP is clearly observed for both projectiles.

Optical model fits were obtained using the searching version of the code FRESKO [27]. Woods-Saxon potentials were used, taking the global ${}^7\text{Li}$ parameters of Cook [28] as a starting point. Good fits were obtained simply by searching on V and W , the real and imaginary potential depths. The potential parameters are given in Table 4, together with the total reaction cross sections deduced from the optical model. As expected, the total reaction cross section for ${}^8\text{B}$ is larger than that for ${}^7\text{Be}$. However, what is unexpected is that it is only $\sim 5\%$ larger; given the order of magnitude smaller breakup threshold for ${}^8\text{B}$ compared to ${}^7\text{Be}$ and the correspondingly much larger expected breakup cross section (see e.g. [19]) it is at first sight surprising that the

Table 1. Woods-Saxon potential parameters for the ${}^7\text{Be}, {}^8\text{B} + {}^{208}\text{Pb}$ elastic scattering plus the corresponding total reaction cross sections.

Reaction system	V	r_V	a_V	W	r_W	a_W	σ_R	χ^2/N
${}^7\text{Be}+{}^{208}\text{Pb}$	114.2	1.286	0.853	12.4	1.739	0.809	3182 mb	1.05
${}^8\text{B}+{}^{208}\text{Pb}$	165.2	1.286	0.853	14.7	1.739	0.809	3342 mb	0.156

difference is not greater. As it is, the two systems have total reaction cross sections that are essentially identical within the likely uncertainties.

This apparently paradoxical behaviour could have several explanations. For incident energies well above the Coulomb barrier—as here—nuclear structure influences on heavy-ion elastic scattering might tend to be “washed out”. This could also explain the very similar elastic scattering angular distributions; if anything, ${}^8\text{B}$ may have the more pronounced CNIP, again unexpected. The similar total reaction cross sections could also point to a much reduced total fusion cross section for ${}^8\text{B}$ compared to ${}^7\text{Be}$ and/or an important contribution from transfer reactions for ${}^7\text{Be}$. More detailed theoretical studies and further experimental data will be needed to elucidate this question.

5. Acknowledgments

We would like to acknowledge all the staff of HIRFL for providing the intense carbon beams and friendly collaboration. This work was partially supported by the Major State Basic Research Development Program of China (973 Program: New physics and technology at the limits of nuclear stability), the Natural Science Foundation of China (NSFC) with Grant Nos. 11075190, 11005127 and 10905076 and the Directed Program of Innovation Project of the Chinese Academy of Sciences with Grant No. KJCX2-YW-N44.

References

- [1] T.Kubo, Nucl. Instr. and Meth. **B204** 97 (2003).
- [2] B.Jonson, Phys. Rep. **389** 1 (2004).
- [3] A.S.Jensen *et al.*, Rev. Mod. Phys. **76** 215 (2004).
- [4] O.Sorlin and M.-G.Porquet, Prog. Part. Nucl. Phys. **61** 602 (2008).
- [5] N.Paar *et al.*, Rep. Prog. Phys. **70** 691 (2007).
- [6] L.F.Canto *et al.*, Phys.Rep. **424** 1 (2006).
- [7] A.M.Sánchez-Benítez *et al.*, Nucl. Phys. **A803** 30 (2008).
- [8] J.P.Fernández-García *et al.*, Nucl. Phys. **A840** 19 (2010).
- [9] A.Di Pietro *et al.*, Phys. Rev. Lett **105**, 022701(2010).
- [10] N.Keeley *et al.*, Phys. Rev. **C82** 034606 (2010).
- [11] Wang Qi *et al.*, Chin. Phys. Lett. **23** 1731 (2006).
- [12] A.Gomez-Camacho *et al.*, Nucl. Phys. **A833** 156 (2010).
- [13] E.F.Aguilera *et al.*, Phys. Rev. Lett. **107** 092701 (2011).
- [14] P.Descouvemout, Phys. Rev. **C70** 065802 (2004).
- [15] F.Schumann *et al.*, Phys. Rev. **C73** 015806 (2006).
- [16] M.H.Smedberg *et al.*, Phys. Lett. **B452** 1 (1999).
- [17] M.M.Obuti *et al.*, Nucl. Phys. **A609** 74 (1996).
- [18] I.Tanihata *et al.*, Phys. Lett. **B206** 592 (1988).
- [19] N.Keeley *et al.*, Prog. Part. Nucl. Phys. **63** 396 (2009).
- [20] I.Pecina *et al.*, Phys. Rev. **C52** 191 (2006).
- [21] G.Tabacaru *et al.*, Phys. Rev. **C73** 025808 (2006).
- [22] E.F.Aguilera *et al.*, Phys. Rev. **C79** 021601(R) (2009).
- [23] A.Barioni *et al.*, Phys. Rev. **C84**, 014603 (2011).
- [24] W.L.Zhan, *et al.*, Sci. Chin. Ser. **A42** 528 (1999).

- [25] Z.Y.Sun *et al.*, Nucl. Instr. and Meth. **A503** 496 (2003).
- [26] J.Rahighi *et al.*, Nucl. Instr. and Meth. **A578** 185 (2007).
- [27] I.J.Thompson, Comput. Phys. Rep. **7** 167 (1988).
- [28] J.Cook, Nucl. Phys. **A388** 153 (1982).